Development of synaptic inhibition in glycine transporter 2 deficient mice

A. Tobias Latal [a,1], Thomas Kremer [b,1,2], Jesús Gomeza [c], Volker Eulenburg [b,d,*,1], Swen Hülsmann [a,e,*,1]

[a] Dept. Neuro- and Sensory Physiology, Center Physiology and Pathophysiology, Georg-August-University Göttingen, Humboldtallee 23, D-37073 Göttingen, Germany
[b] Department of Neurochemistry, Max Planck Institute for Brain Research, Deutschordenstrasse 46, 60529 Frankfurt, Germany
[c] Institute for Pharmaceutical Biology, Nußallee 6, 53115 Bonn, Germany
[d] Institute for Biochemistry and Molecular Medicine, University of Erlangen, Fahrstrasse 17, 91054 Erlangen, Germany
[e] DFG-Research Center for Molecular Physiology of the Brain, 37073 Göttingen, Germany

Introduction

In the central nervous system, fast inhibitory neurotransmission is mediated by glycine and γ-aminobutyric acid receptors (GABA), acting on postsynaptic glycine receptors (GlyR) or A-subtype γ-aminobutyric acid receptors ($GABA_AR$) that open intrinsic receptor-linked anion channels. Depending on the intracellular chloride concentration, channel opening inhibits the postsynaptic cell by hyperpolarisation or by shunting inhibition.

Both transmitter systems share some key components, such as the postsynaptic scaffolding protein gephyrin or the vesicular inhibitory amino acid transporter VIAAT (Kneussel and Loebrich, 2007; Wojcik et al., 2006). The overlap of such key components at many inhibitory synapses in the spinal cord and brainstem results in the occurrence of both GlyR and $GABA_AR$ mediated inhibitory postsynaptic currents (IPSCs) at individual synapses (Jonas et al., 1998; Lu et al., 2008; Muller et al., 2006; O'Brien and Berger, 1999; Singer and Berger, 2000) that differ in their kinetic and pharmacological properties. The dual-component nature of unitary IPSCs has been attributed to quantal co-release of glycine and GABA from single vesicles (Jonas et al., 1998), linked to simultaneous loading of both transmitters into synaptic vesicles by the vesicular inhibitory amino acid transporter (VIAAT). A deficiency in VIAAT results in drastic reduction of GABA and glycine release from inhibitory nerve terminals (Wojcik et al., 2006), suggesting that both transmitters compete for VIAAT mediated vesicle loading (Burger et al., 1991; Christensen and Fonnum, 1991; Christensen et al., 1991; Rousseau et al., 2008).

Several marker proteins in GABAergic presynaptic terminals have been identified that are necessary for efficient GABAergic neurotransmission, including the GABA synthesizing enzymes GAD65 and GAD67 and the GABA transporter GAT1. At present, only the glycine transporter GlyT2 has been recognized as a reliable marker for glycinergic presynaptic terminals. GlyT2 is targeted specifically to the plasma membrane surrounding the presynaptic specializations (Mahendrasingam et al., 2000; Zafra et al., 1995). GlyT2 deficiency in mice ($GlyT2^{-/-}$) produces a complex neuromotor phenotype including hind feet clasping, spasticity, spontaneous tremors and an impaired righting response, followed by premature death during the second postnatal week (Gomeza et al., 2003b). The phenotype seen in

* Corresponding authors. V. Eulenburg is to be contacted at Institute for Biochemistry and Molecular Medicine, University of Erlangen, Fahrstrasse 17, 91054 Erlangen, Germany. Tel.: +49 9131 8526206; fax: +49 9131 8522485. S. Hülsmann, Abt. Neuro- und Sinnesphysiologie, Zentrum Physiologie und Pathophysiologie, Georg-August-Universität Göttingen, Humboldtallee 23, D-37073 Göttingen, Germany. Tel.: +49 551 399592; fax: +49 551 399676.

E-mail addresses: volker.eulenburg@biochem.uni-erlangen.de (V. Eulenburg), shuelsm2@uni-goettingen.de (S. Hülsmann).

[1] These authors contributed equally to the study.

[2] Present address: Hoffmann-La-Roche Ltd, Pharmaceutical Research Neuroscience, CH-4070 Basel.

GlyT2$^{-/-}$ mice mimics most of the symptoms seen in human hyperekplexia patients. Mutations in the GlyT2 gene have recently been identified in human hyperekplexia patients, suggesting that GlyT2 is one of the genes associated with the disease (Eulenburg et al., 2006; Rees et al., 2006). Similar to other genetic defects resulting in hyperekplexia-like symptoms such as mutations in the GlyR α1 or β subunit (Rees et al., 2002; Shiang et al., 1993), the phenotype seen in GlyT2$^{-/-}$ mice was attributed to marked reduction in glycinergic inhibitory postsynaptic currents leading to disinhibition of motoneurons. Since major changes in GlyR clustering and/or expression were excluded, it has been proposed that GlyT2 is essential for the reuptake and proper reincorporation of glycine into presynaptic glycinergic nerve terminals (Gomeza et al., 2003b). Although GlyT2 is already expressed during late embryonic development (E16–17), GlyT2 deficient mice do not show symptoms in early postnatal development (P0–P4).

To identify the ontogenetic onset of the failure of glycinergic transmission and to clarify whether the decrease in the levels of presynaptic glycine significantly affects the content of GABA in synaptic vesicles, we analyzed glycinergic and GABAergic synaptic transmission in GlyT2$^{-/-}$ and wild-type (WT) animals.

Results

Glycine content of presynaptic terminals is reduced in newborn GlyT2$^{-/-}$ mice

In postnatal (P0–P4) mice, GlyT2 deficiency does not result in any detectable phenotype, as tested by simple handling assays that reveal hypereklexia like symptoms in GlyT2$^{-/-}$ mice (Gomeza et al., 2003b). It is possible that at this developmental stage, de-novo synthesis of glycine (Daly and Aprison, 1974) or GlyT2 independent glycine uptake allows for efficient loading of synaptic vesicles. Therefore, we tested whether normal glycine concentration is present in presynaptic terminals of GlyT2 deficient mice during the first postnatal week. Glycine accumulation was measured immunohistochemically with an antibody raised against a paraformaldehyde conjugate of glycine (Pow et al., 1995). First, we stained brainstem and spinal cord slices of P10 WT and age-matched GlyT2$^{-/-}$ mice. In both regions of WT animals, there was a strong labelling of presumptive glycinergic presynaptic terminals. In contrast, immunoreactivity was strongly reduced in sections from GlyT2$^{-/-}$ mice (Fig. 1A and Table 1). As shown previously, this reduction is not caused by a loss of inhibitory

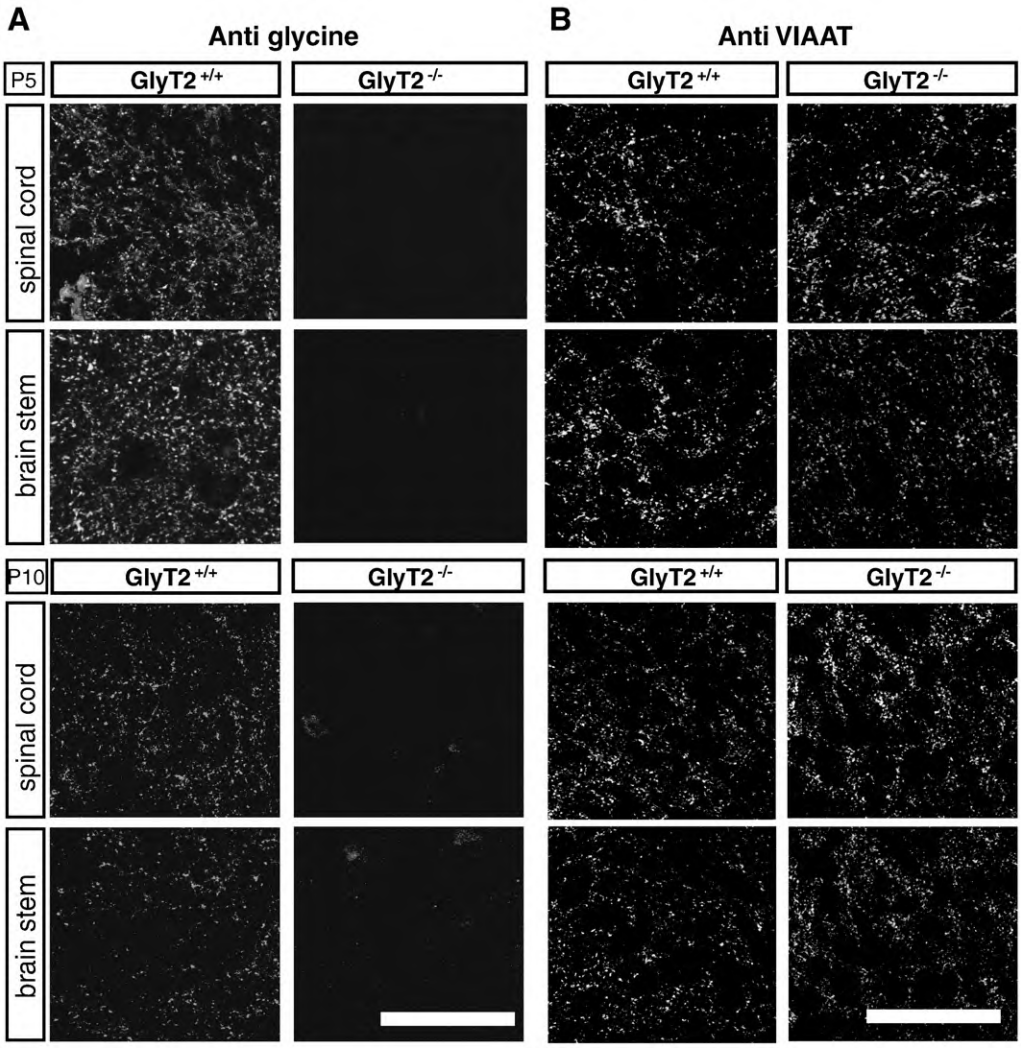

Fig. 1. Reduction of glycincie immunoreactivity in sections of GlyT2$^{-/-}$ mice. Brainstem and spinal cord of GlyT2$^{-/-}$ mice and WT littermates were dissected at P5 and P10 and stained after fixation with antibodies against glycine (A) and VIAAT (B). Note that in sections from GlyT2$^{-/-}$ mice the anti-glycine staining was nearly completely lost, whereas the VIAAT staining, indicative for inhibitory presynaptic terminals was indistinguishable from that seen in WT section (scale bar represents 20 μm).

Table 1
Quantification of immunreactive signals for markers of inhibitory synapses in brainstem derived from animals with the indicated age and genotype.

	P0		P5		P10	
	+/+	−/−	+/+	−/−	+/+	−/−
Glycine	111 ± 9	11 ± 6	120 ± 20	10 ± 8	135 ± 28	10 ± 6
VIAAT	141 ± 24	158 ± 28	165 ± 23	177 ± 46	212 ± 21	210 ± 32
Gephyrin	223 ± 31	228 ± 36	226 ± 29	220 ± 34	287 ± 51	320 ± 44
GABA	93 ± 23	86 ± 18	88 ± 15	102 ± 25	47 ± 18	56 ± 18
GAD65	99 ± 8	108 ± 11	83 ± 28	87 ± 29	70 ± 11	74 ± 23
GAD67	85 ± 13	89 ± 18	71 ± 15	56 ± 22	56 ± 13	61 ± 9

Values were determined on brainstem sections stained with the indicated antibodies manually as immunreactive puncta (>0.7 μm) per 1000 μm^2 tissue. Data represent means ± SD ($n \geq 4$). For each staining, at least 1000 immunreactive clusters were counted (with the exception of the glycine staining in the GlyT2$^{-/-}$ mice).

synapses, since VIAAT immunoreactivity was indistinguishable from that seen in WT sections (Fig. 1B and Table 1, see also Gomeza et al., 2003b). The majority of immunoreactive clusters correspond to inhibitory synapse specializations, as revealed by colabelling of VIAAT with a gephyrin specific antibody (data not shown). The reduced immunoreactivity in GlyT2$^{-/-}$ mice is consistent with electrophysiological studies (Gomeza et al., 2003b) and shows that GlyT2 gene inactivation results in a drastic reduction of presynaptically accumulated glycine.

The dramatic reduction of glycine staining was also observed in GlyT2$^{-/-}$ mice during the first postnatal week. At P0 (Table 1) and P5 (Fig. 1 and Table 1), glycine staining in GlyT2$^{-/-}$ spinal cord and brainstem sections was reduced by 90% as compared to WT littermates, without affecting the number of VIAAT/gephyrin-colabled clusters. It appears that glycine de-novo synthesis or its uptake by GlyT2 independent transport systems is not sufficient to compensate for the loss of GlyT2 at any time during postnatal development.

Electrophysiological evidence for depression of glycinergic neurotransmission in newborn GlyT2$^{-/-}$ mice

To investigate whether the apparent loss of presynaptic glycine coincides with the onset of defects in glycinergic synaptic transmission in the newborn mice, we measured amplitude and frequency of glycinergic inhibitory postsynaptic currents (IPSC$_{gly}$) in hypoglossal motoneurons from WT and GlyT2$^{-/-}$ mice, in brainstem slice preparations at three different stages of postnatal development (Fig. 2).

Similar to our earlier observation (Gomeza et al., 2003b), glycinergic spontaneous IPSCs (sIPSC$_{gly}$) were reduced in P6 to P8 GlyT2$^{-/-}$ animals compared to their WT littermates. The sIPSC$_{gly}$ amplitude in GlyT2$^{-/-}$ hypoglossal motoneurons was 37.1 ± 16.3 pA ($n = 9$) whereas the average amplitude was 77.2 ± 49.6 pA ($n = 7$) in WT cells ($p \leq 0.05$). The sIPSC$_{gly}$ frequency in GlyT2$^{-/-}$ neurons was somewhat smaller compared to WT cells (GlyT2$^{-/-}$: 8.1 ± 11.0 Hz vs. WT: 15.3 ± 5.9 Hz, n.s).

In slices from younger (P3–P5) WT animals, the sIPSC$_{gly}$ amplitude was slightly smaller (59.2 ± 28.2 pA; $n = 15$) than P6–8 WT animals. In P3–P5 GlyT2$^{-/-}$ mice sIPSC$_{gly}$ amplitudes were significantly reduced (29.7 ± 12.1 pA; $n = 6$; $p \leq 0.05$). In these recordings the sIPSC$_{gly}$ frequency in GlyT2$^{-/-}$ mice was slightly but not significantly reduced (GlyT2$^{-/-}$: 4.5 ± 4.8 Hz vs. WT: 11.9 ± 9.7 Hz; n.s.).

Notably, a strong reduction of sIPSC$_{gly}$ amplitude was already apparent in GlyT2$^{-/-}$ newborn mice (P0–P2) that however, were phenotypically indistinguishable from WT animals. Here, recordings from hypoglossal motoneurons of GlyT2$^{-/-}$ mice revealed a massive reduction of the sIPSC$_{gly}$ amplitude to less than 50% of the WT controls (GlyT2$^{-/-}$: 23.7 ± 5.1 pA; $n = 11$ vs. WT: 53.3 ± 27.8 pA; $n = 5$; $p \leq 0.05$). At this early developmental stage, the reduction of sIPSC$_{gly}$ frequency was significant (GlyT2$^{-/-}$: 1.1 ± 0.9 Hz vs. WT: 7.1 ± 6.7 Hz; $p \leq 0.05$).

Postnatal change of sIPSC$_{gly}$ decay kinetics is normal in GlyT2$^{-/-}$ mice

It is known that the subunit composition of glycine receptors changes during postnatal development (Singer et al., 1998). In a previous study, we excluded major postnatal changes in GlyRα1 and GlyRα2 expression in GlyT2$^{-/-}$ mice using an immunohistochemical approach (Gomeza et al., 2003b). In the present study, we used more precise electrophysiological methods of analysis. We analyzed sIPSC$_{gly}$ kinetics in WT and GlyT2$^{-/-}$ neurons at different postnatal stages (Fig. 2). At P0–P2, the decay time constant (τ_{decay}) of sIPSC$_{gly}$ of WT mice was 13.6 ± 3.6 ms ($n = 5$), and gradually decreased with age: 12.0 ± 5.8 ms at P3–P5 ($n = 15$), 11.8 ± 4.5 ms at P6–P8 ($n = 27$) and 7.2 ± 1.1 ms at the end of the second postnatal week (P12–14; $n = 30$), the latter being significantly reduced compared to the earlier postnatal stages ($p \leq 0.05$).

A similar age dependent reduction of τ_{decay} was observed in recordings from GlyT2$^{-/-}$ neurons: At P0–P2, 17.5 ± 5.9 ms ($n = 10$); at P3–P5, 12.3 ± 4.9 ms ($n = 6$); at P6–P8, 11.3 ± 3.6 ms, ($n = 9$); $p \leq 0.05$. Values of τ_{decay} in GlyT2$^{-/-}$ neurons were not significantly different from the age-matched WT neurons. We were unable to record from GlyT2$^{-/-}$ mice at P12–P14 because the mice died earlier. The electrophysiological measurements further strengthen our contention that GlyT2 gene inactivation does not lead to changes in GlyR expression or subunit composition in the first postnatal week, although glycinergic neurotransmission is functionally impaired.

GABAergic neurotransmission is not up-regulated in GlyT2 deficient mice

In cell culture experiments, pharmacological blockade of GlyT2 up-regulates GABA release, presumably due to the reduction of glycine competition at the VIAAT (Rousseau et al., 2008). Since in GlyT2$^{-/-}$ mice presynaptic glycine levels appear to be reduced, we investigated whether GABAergic neurotransmission is up-regulated.

Direct visualization of GABA with a specific antibody did not reveal increased presynaptic accumulation of GABA in brainstem or spinal cord slices of GlyT2$^{-/-}$ mice (Fig. 3 and Table 1). GABA content in symptomatic GlyT2$^{-/-}$ mice (P10) was comparable to that seen in WT animals in both regions analyzed. We also looked for changes in GABA immunoreactivity at earlier postnatal stages, since the number of GABAergic terminals decreases in brainstem and spinal cord during early postnatal development (Muller et al., 2006). At P0 and P5, the number of immunoreactive puncta was almost doubled compared to P10 (Table 1). However we did not detect differences between sections from WT and GlyT2$^{-/-}$ mice (Fig. 3 and Table 1).

To measure functional GABAergic neurotransmission in WT and GlyT2$^{-/-}$ animals, we recorded spontaneous GABAergic currents (sIPSC$_{GABA}$, Fig. 4). At P6–P8, when a mild form of the GlyT2$^{-/-}$ phenotype is behaviourally apparent, sIPSC$_{GABA}$ amplitude was 35.0 ± 9.7 pA ($n = 8$) in WT and 41.3 ± 16.5 pA in GlyT2$^{-/-}$ littermates ($n = 8$; n.s.). Frequency of sIPSC$_{GABA}$ in WT mice was 12.4 ± 11.0 Hz and in GlyT2$^{-/-}$ mice, 11.9 ± 6.6 Hz (n.s.). Decay time constants were likewise similar (GlyT2$^{-/-}$: 25.5 ± 7.6 ms; WT: 28.6 ± 8.9 ms; n.s).

In younger animals (P3–P5), of both genotypes, the amplitude of the sIPSC$_{GABA}$ was indistinguishable (GlyT2$^{-/-}$: 40.4 ± 10.4 pA; $n = 8$ vs. WT: 37.9 ± 18.3 pA; $n = 6$; n.s). In addition, sIPSC$_{GABA}$ frequencies were not changed (GlyT2$^{-/-}$: 3.5 ± 4.2 Hz vs. WT: 5.0 ± 3.3 Hz, n.s.) and τ_{decay} of GABAergic sIPSCs were similar in GlyT2$^{-/-}$mice (44.7 ± 21.4 ms) and WT mice (38.1 ± 18.4 ms; n.s.).

At P0–P2, sIPSC$_{GABA}$ amplitude was 33.6 ± 10.2 pA ($n = 6$) in GlyT2$^{-/-}$ neurons and 28.6 ± 8.6 pA ($n = 7$; n.s,) in WT neurons. There was also no significant difference between genotypes in sIPSC$_{GABA}$ frequency (GlyT2$^{-/-}$: 1.5 ± 0.9 Hz vs. WT: 2.2 ± 3.2 Hz) or in τ_{decay} (68.7 ± 21.2 ms in GlyT2$^{-/-}$ mice, 47.5 ± 23.3 ms in WT).

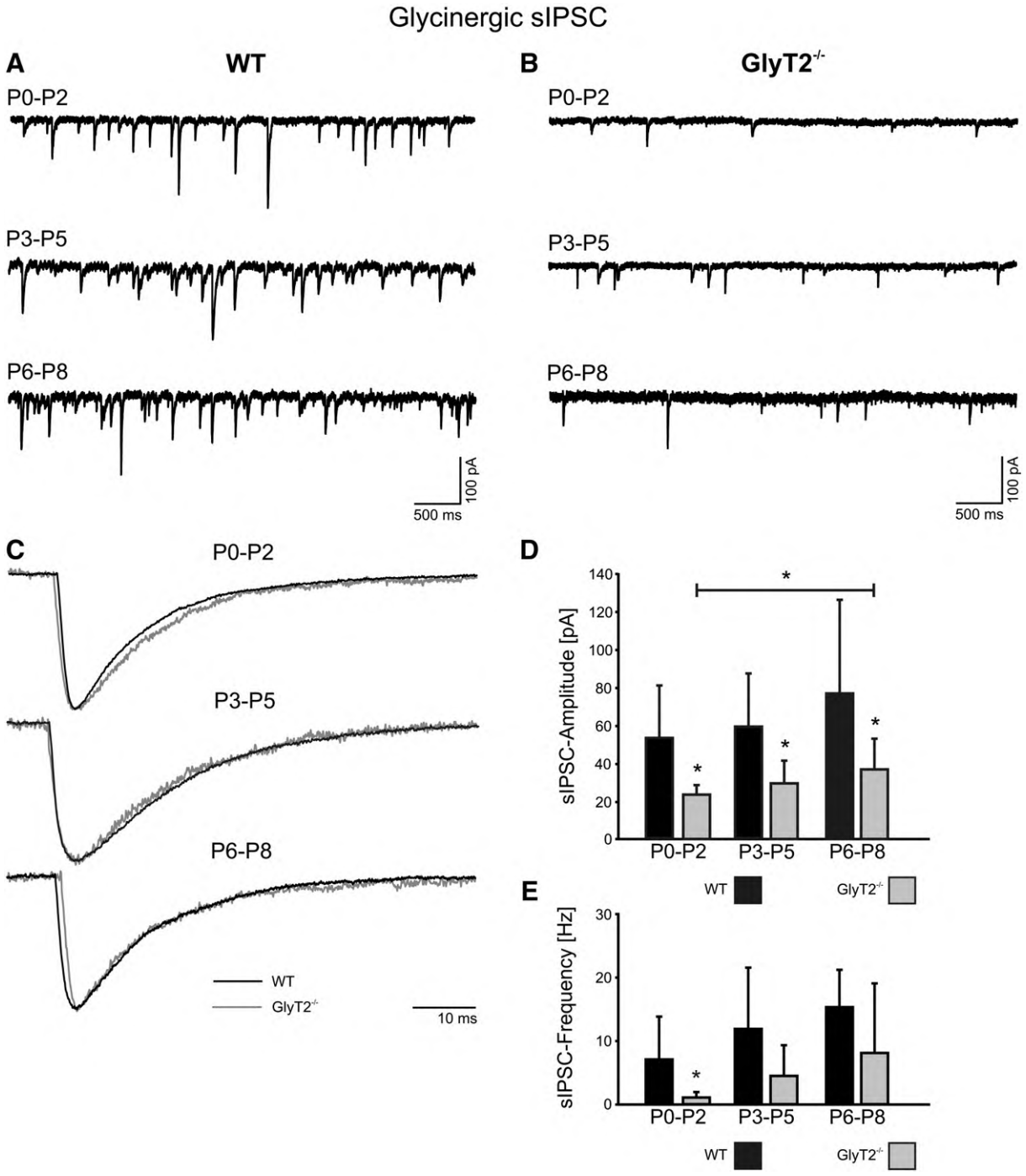

Fig. 2. Glycinergic neurotransmission is already impaired in presymptomatic GlyT2 deficient mice. A, B: glycinergic IPSCs of hypoglossal motoneurons at different stages of postnatal development: comparison of recordings from WT mice (A) and GlyT2$^{-/-}$ mice (B). C: Normalized average waveforms of spontaneous glycinergic IPSC from hypoglossal motoneurons of WT and GlyT2$^{-/-}$ mice. D, E: Average amplitudes (D) and frequencies (E) of spontaneous IPSC$_{gly}$ from WT and GlyT2$^{-/-}$ mice (±SD). The asterisks indicate significant changes. Data were obtained in the presence of 100 μM AP-5, 20 μM CNQX and 20 μM bicuculline.

Saturation of postsynaptic GABA$_A$ receptors during GABA release events might mask an increased GABA release in GlyT2$^{-/-}$ preparations. We therefore tested for GABA$_A$ receptors saturation measuring evoked GABAergic IPSC (eIPSC$_{GABA}$) in paired-pulse-stimulation-experiments (Fig. 5). Supra maximal stimulation resulted in comparable eIPSC$_{GABA}$ amplitudes in WT and GlyT2$^{-/-}$ mice (WT: 1.1 nA ± 0.7 nA; $n=4$; vs. GlyT2$^{-/-}$: 1.0 ± 0.5 nA; $n=5$; n.s.). At a stimulus interval of 25 ms (Fig. 5A, B, bottom traces), the eIPSC$_{GABA}$ evoked by the second pulse arises at a time point when GABA$_A$ receptors are still activated by GABA released upon the first stimulus. An increase of the peak current after the second pulse occurred in both WT and GlyT2$^{-/-}$ mice, revealing no difference between the genotypes. In both genotypes the 2-fold increase of the peak current after the second stimulus indicates that GABA$_A$ receptors were not saturated by GABA released by the first pulse. The ratio $a2_{total}/a1$ (see Experimental methods) was 2.0 ± 0.5 ($n=4$) in WT and 2.1 ± 0.5; $n=5$; in GlyT2$^{-/-}$ mice (n.s., Fig. 5D).

Enhanced presynaptic GABA release from GlyT2$^{-/-}$ neurons could increase presynaptic auto-inhibition via GABA$_B$ receptors, and activation of GABA$_B$ receptors increases paired-pulse facilitation (PPF; Tanabe

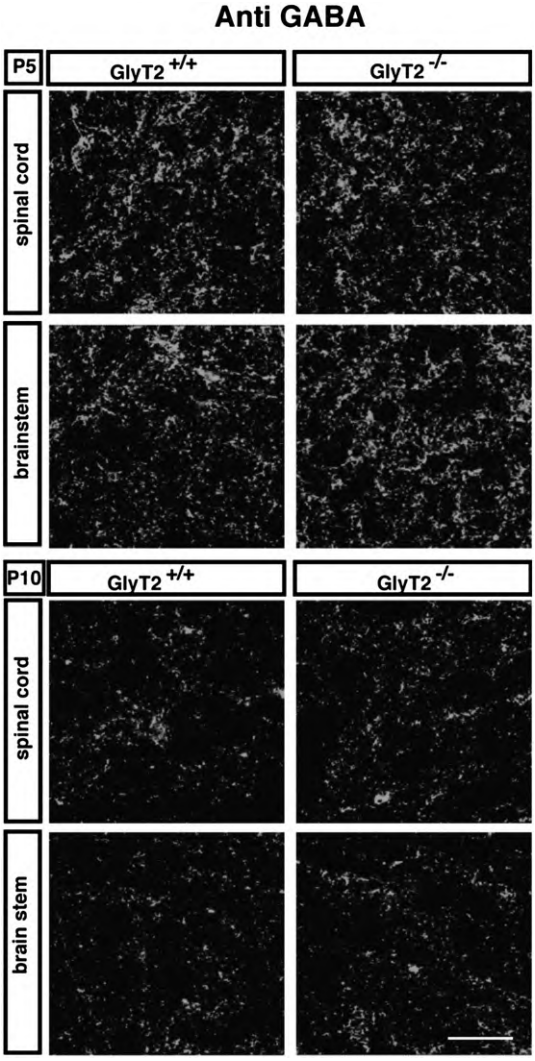

Fig. 3. GlyT2 gene inactivation does not lead to impaired GABA accumulation in brainstem and spinal cord. Brainstem and spinal cord of GlyT2$^{-/-}$ mice and WT littermates were dissected at the age indicated and after fixation and sectioning stained with antibodies against GABA (scale bar represents 20 μm).

and Kaneko, 1996). To test this possibility, we performed paired-pulse experiments at stimulus frequencies of 2.5 to 40 Hz with supra maximal stimuli. Generally the paired-pulse ratio ($a2/a1$) was very variable and a significant PPF was only observed at 10 Hz in both WT and GlyT2$^{-/-}$ mice (Fig. 5). At all other stimulation frequencies, no significant PPF was detectable. However, no differences of the paired-pulse ratio between WT (1.12 ± 0.1; $n = 4$) and GlyT2$^{-/-}$ (1.17 ± 0.1; $n = 5$; n.s.) was observed at 10 Hz nor at any other stimulation frequency.

GABAergic unitary release events are not increased in GlyT2$^{-/-}$ mice

Spontaneous IPSCs as well as evoked IPSCs depend on the electrical activity of the presynaptic cell. To test if significant changes of GABAergic transmission in GlyT2$^{-/-}$ mice were missed when analysing spontaneous IPSCs, we recorded GABAergic miniature IPSCs in P3–P5 WT and GlyT2$^{-/-}$ mice (Fig. 6). Unitary IPSC (mIPSC$_{GABA}$) amplitudes did not differ significantly between both genotypes (GlyT2$^{-/-}$: 19.4 ± 5.5 pA; $n = 8$; vs WT: 18.0 ± 4.4 pA; $n = 10$; n.s.). In addition, mIPSC$_{GABA}$ frequency was not altered (GlyT2$^{-/-}$: 1.5 ± 0.9 Hz vs. WT: 1.3 ± 1.6 Hz; n.s.). GABAergic mIPSC decay kinetics tended to be slower in recordings from GlyT2$^{-/-}$ slices compared to WT preparations (GlyT2$^{-/-}$: 55.4 ± 15.5 ms vs. WT: 41.6 ± 17.4 ms), but the difference was not significant.

The electrophysiological findings are consistent with the immunochemical data and indicate that the strong reduction of glycinergic neurotransmission is not accompanied by a significant up-regulation of GABAergic neurotransmission in GlyT2$^{-/-}$ mice.

GlyT2$^{-/-}$ mice show normal synaptic protein expression of the GABAergic system

To determine whether the failure of GlyT2$^{-/-}$ neurons to increase GABAergic transmission might be related to additional changes in synaptic protein expression of the GABAergic system in the GlyT2$^{-/-}$ mice line, we quantified the immunoreactivity of the glutamate decarboxylases GAD65 and 67 in brain stem and spinal cord sections (see Fig. 7A and Table 1). We did not recognize any change of GAD65 or 67 distributions in sections from GlyT2$^{-/-}$ mice as compared to parallel processed WT brainstem and spinal cord sections at all postnatal stages analyzed (P0, P5 and P10). This indicates that localization and/or expression of these GABA synthesizing enzymes is not changed in GlyT2$^{-/-}$ mice.

Another source of intracellular GABA is the plasma membrane transporter GAT1, which is predominantly localized in the presynaptic terminal (Conti et al., 1998; Minelli et al., 1995). To investigate whether GlyT2 deficiency leads to adaptive changes in GAT1 activity, we analyzed expression and transport activity of GAT1. GAT1 specific uptake activity was analysed as the tiagabine sensitive fraction of total GAT activity in P2 membrane preparations. GAT1-dependent GABA uptake was indistinguishable in membrane preparations from brainstem and spinal cord of WT and GlyT2$^{-/-}$ mice at all ages investigated (P0, P5, P10; Fig. 7B). Total GAT1 protein expression was also not different in GlyT2$^{-/-}$ mice (Fig. 7C and Table 2), thus excluding changes in GABA uptake capacity of the presynaptic terminals, as a consequence of GlyT2 deficiency.

Discussion

The present study focussed on two important aspects of synaptic inhibition. We investigated how GlyT2 deficiency alters glycinergic transmission during early postnatal development, and we determined whether competition of GABA and glycine for VIAAT-dependent vesicular filling represents a physiological mechanism to compensate for the loss of glycine uptake in GlyT2$^{-/-}$ mice.

GlyT2$^{-/-}$ mice are born with a strong reduction of glycinergic transmission

By an immunohistochemical approach we demonstrated that glycine labelling of glycinergic presynaptic terminals is strongly reduced, suggesting that the reduction of glycinergic transmission seen in recordings from GlyT2 deficient mice is caused by an insufficient reuptake of glycine via GlyT2 as hypothesized earlier (Gomeza et al., 2003b). From an analysis of glycinergic IPSC kinetics, we propose that no other more subtle adaptive mechanisms related to glycine receptor function contribute to the phenotype seen in GlyT2 deficient mice. This is consistent with previous findings showing normal GlyR expression at silent glycinergic synapses (Mangin et al., 2002), and can now be extended to fully functional synapses. Apparently, reduced glycine uptake into the glycinergic presynaptic terminal in GlyT2$^{-/-}$ mice cannot be compensated for by de-novo glycine synthesis or by low affinity uptake systems. Thus, without GlyT2, inhibitory neurons cannot maintain the high cytosolic glycine concentrations that are required for adequate loading of vesicles.

Neonatal GlyT2$^{-/-}$ mice are apparently normal at birth, although there might be a very mild form of the phenotype that, for example, involves impaired tongue movements. Gross hypoglossal motor output, however, is normal, since no respiratory or feeding phenotype is

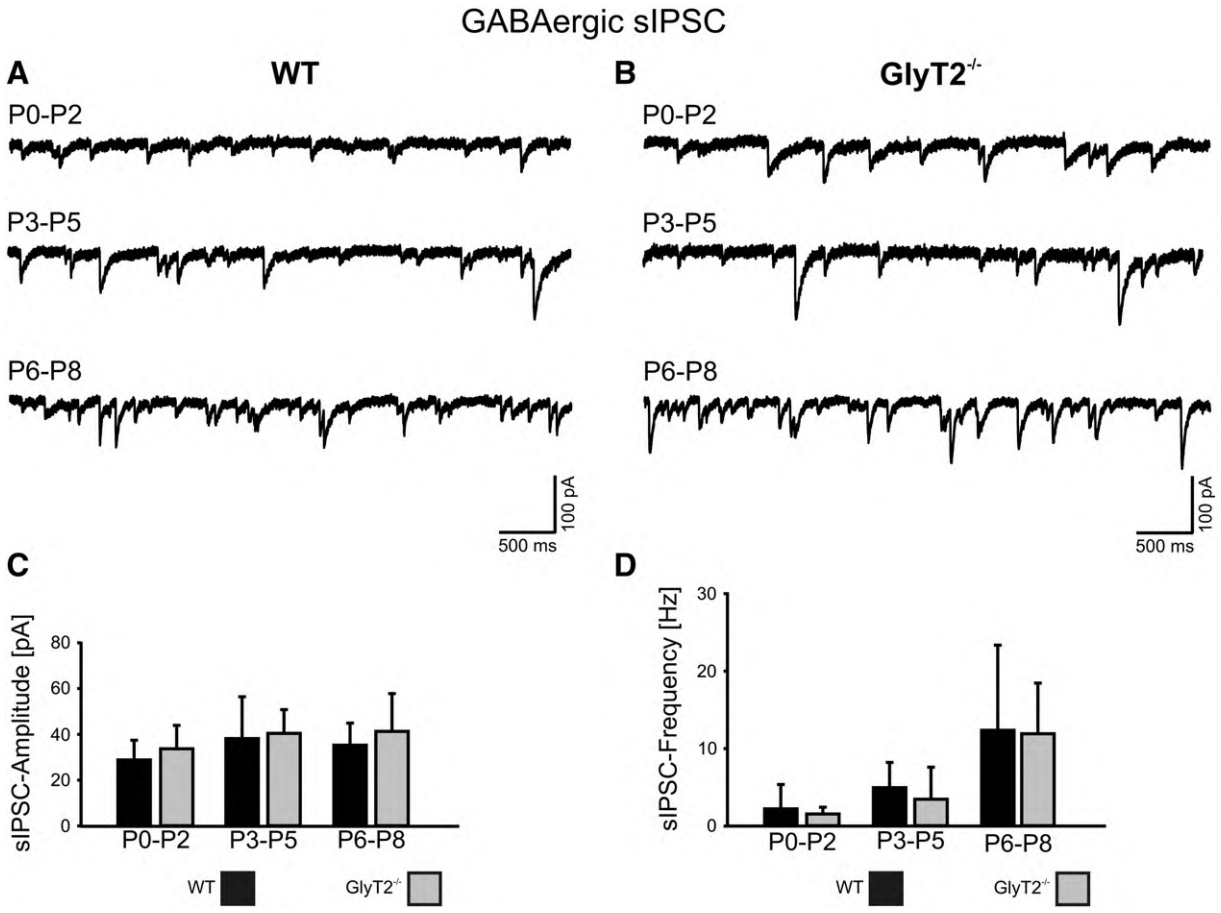

Fig. 4. Spontaneous GABAergic IPSCs are unchanged in GlyT2 deficient mice. A, B: Spontaneous GABAergic postsynaptic currents of hypoglossal motoneurons at different stages of postnatal development. Wild-type mice (WT, A) compared to GlyT2 knockout mice (GlyT2$^{-/-}$, B). C, D: Average amplitudes (C) and frequencies (D) of identified spontaneous $IPSC_{GABA}$ from WT and GlyT2$^{-/-}$ mice. Data were obtained in the presence of 100 μM AP-5, 20 μM CNQX and 10 μM strychnine.

observed in animals of this age. This contrasts with our results obtained by immunohistochemical and electrophysiological analysis in young GlyT2 deficient mice, which revealed pronounced disturbances of glycinergic synaptic function in animals prior to the onset of the phenotype.

Postnatal changes of glycinergic transmission

The appearance of symptoms at the end of the first postnatal week coincides with changes of the chloride equilibrium potential. It is known that glycine induces depolarising postsynaptic potentials in hypoglossal motoneurons at early developmental stages (P0–P3; Singer et al., 1998). Moreover in the lumbal spinal motoneurons (P1–P3) the equilibrium potential for chloride mediated postsynaptic currents is also depolarising at birth and shifts toward hyperpolarisation by the end of the first postnatal week (Stil et al 2009). Thus, the depolarising nature of glycinergic postsynaptic potentials might be involved in the delay of a phenotype of the GlyT2$^{-/-}$ mice, during the first days of life. Against these hypotheses argues that some inhibitory action of glycine (presumably via shunting inhibition) is already seen in newborn animals. Here the loss of the Glycine transporter 1 (GlyT1) results in extracellular accumulation of glycine causing severe symptoms of over-inhibition including a flaccid motor phenotype and abnormal respiratory activity (Gomeza et al. 2003a). Moreover, the blockade of glycinergic receptors by systemic application of the glycine receptor antagonist strychnine leads to severe symptoms of over-excitation and spasticity already in neonatal mice (P0) thus corroborating an important inhibitory function of glycine already at that age (Feng et al., 1998).

No GABAergic compensation occurs in GlyT2$^{-/-}$ mice

In caudal regions of the CNS the analysis of mIPSC decay kinetics has shown that 35–44% of all inhibitory synapses release both glycine and GABA in early postnatal development (Jonas et al., 1998; Muller et al., 2006). At later developmental stages, however, this is reduced to 12% of all inhibitory synapses (Muller et al., 2006). Both transmitters are incorporated via the VIAAT into the synaptic vesicle and thus allowing their simultaneous release from individual vesicles (Burger et al., 1991; Chaudhry et al., 1998; Christensen and Fonnum, 1991; Christensen et al., 1991; McIntire et al., 1997; Sagne et al., 1997). Thus GABA and glycine most likely compete for the vesicular uptake (Christensen et al., 1991), and after inhibition of GlyT2 or loss of GlyT2 expression GABA loading should be subsequently up-regulated. Indeed pharmacological blockade of GlyT2 in cultured spinal cord neurons results in a reduction of glycine release and increase of GABA release in response to presynaptic electrical stimulation (Rousseau et al., 2008).

In our study, however, mice with genetic ablation of GlyT2 expression did not exhibit a detectable increase in vesicular GABA concentration at any developmental stage analysed. Moreover, in GlyT2$^{-/-}$ mice, changes of the expression or function of key components of GABAergic synapses, e.g. GAD65, GAD67 or GAT1 that counteract the compensatory vesicular GABA loading in GlyT2$^{-/-}$ mice, were not evident.

To test whether saturation of postsynaptic $GABA_A$ receptor masked a change of GABA release we analyzed accumulation of GABA in the synaptic cleft by high frequency (40 Hz) paired-pulse stimulation. Here, the increase in the total eIPSC amplitude after the second stimulus

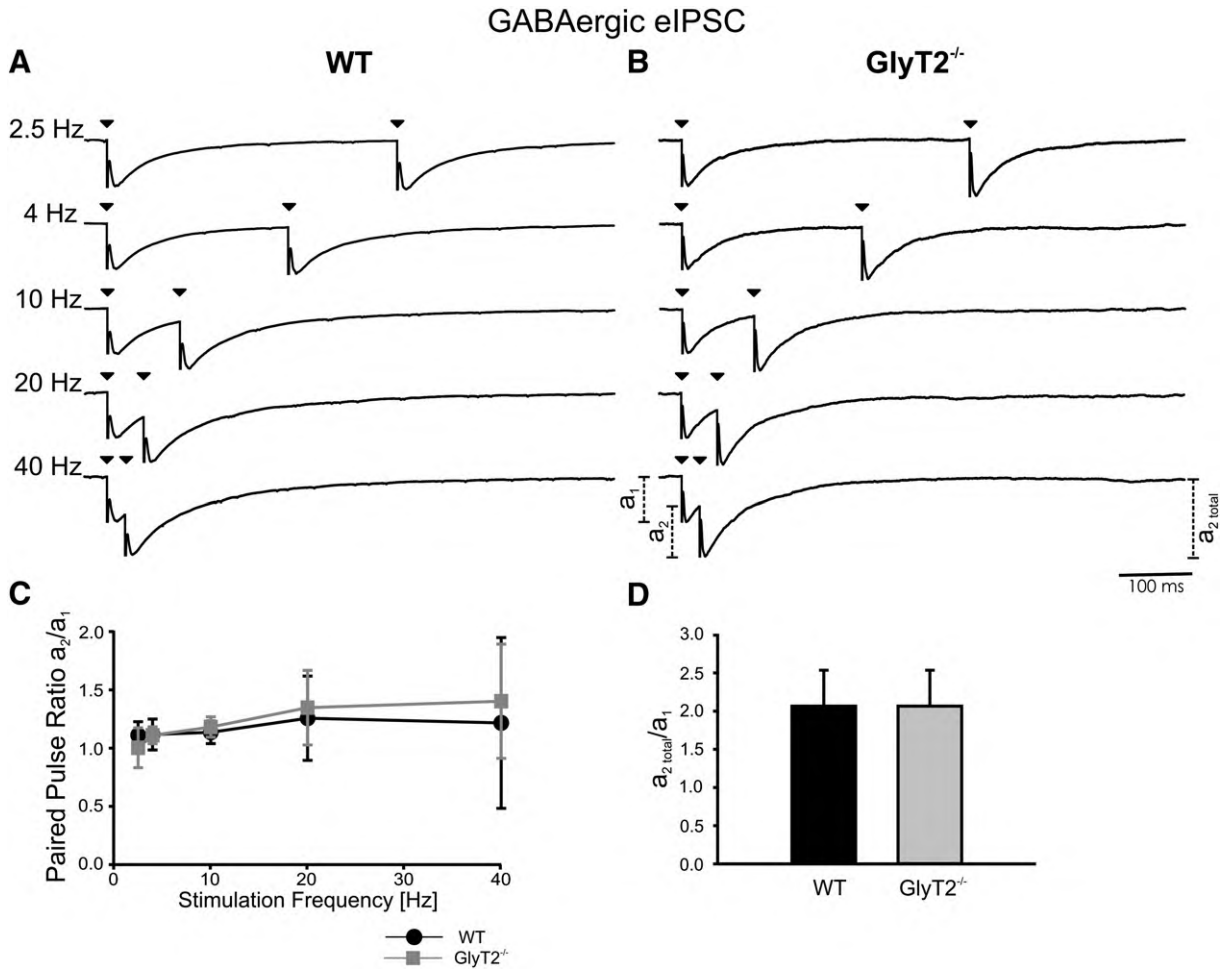

Fig. 5. No change in paired-pulse facilitation and $GABA_A$ receptor occupancy in $GlyT2^{-/-}$ mice after evoked GABA release. A, B: Evoked GABAergic IPSC after presynaptic stimulation (P5–P6 WT (A) and $GlyT2^{-/-}$ mice (B), 2.5–40 Hz stimulation frequency). Traces were normalized to unitary amplitudes after the first stimulus. C: Average ratios of the eIPSC amplitudes after the second to that after the first stimulus in WT and $GlyT2^{-/-}$ mice. At 10 Hz a significant paired-pulse facilitation can be observed in WT and $GlyT2^{-/-}$ mice, which is not significantly different between these two genotypes. D: The average ratio of the total amplitude after the second to the amplitude after the first stimulus (40 Hz). In both genotypes maximal half of the postsynaptic $GABA_A$ receptors were activated after the first stimulus. There is no difference between the a_{total}/a_1 ratios in both genotypes. Solution contained 100 μM AP-5, 20 μM CNQX and 10 μM strychnine.

indicates that more $GABA_A$ receptors can be recruited after the first GABA release. Therefore it is unlikely that postsynaptic $GABA_A$ receptors were saturated after single evoked GABA release events. Due to the experimental procedure with supra maximal stimuli we assume that the same population of synapses was activated after both stimuli. However we cannot exclude the recruitment of additional synapses contributing to the increased amplitude after the second stimulus.

Additionally we demonstrated that GlyT2 deficiency does not result in changes in the presynaptic GABA release probability e.g. by increased presynaptic $GABA_B$ receptor activation (Mintz and Bean, 1993; Misgeld et al., 1995; Zhang et al., 2002) since no change in paired-pulse-facilitation (Tanabe and Kaneko, 1996) was observed in the recordings from $GlyT2^{-/-}$ mice.

Our study suggests that control-mechanisms additional to the presynaptic transmitter concentrations are responsible for the differential loading of GABA and glycine into individual synaptic vesicles. One possibility is that the complex formation of GAD65 with VIAAT (Jensen et al., 2003; Jin et al., 2003) is a prerequisite for VIAAT mediated incorporation of GABA into synaptic vesicles. These additional regulatory mechanisms might develop during the early postnatal development and might not occur in the culture system used by Rousseau et al. (2008). Clearly, more experiments are required to resolve the precise mechanism how VIAAT specificity is regulated at mixed inhibitory synapses.

Taken together, our data show that the massive reduction of glycinergic neurotransmission at all developmental stages, is not compensated by an enhanced filling of synaptic vesicles with GABA.

Experimental methods

Electrophysiology

Electrophysiological experiments were performed on medullary slice preparations from $GlyT2^{-/-}$ mice and WT littermates. Genotyping was performed as described previously (Gomeza et al., 2003b). Animals used in this study were acquired and treated in accordance with the guidelines of the German Physiological Society as well as federal regulations. Neonatal mice were rapidly killed by decapitation. The brains were removed from the skull, the isolated brainstem was placed in carbogen-saturated (95% O_2, 5% CO_2) ice-cold artificial cerebrospinal fluid (aCSF; see below for composition). Transverse slices (280–310 μm) were cut with a vibratome (Leica, Wetzlar, Germany) at the level of the caudal end of the fourth ventricle to include the nucleus of the hypoglossal nerve. Slices were stored in aCSF at room temperature for at least 30 min before starting an experiment and subsequently transferred to a recording chamber and kept submerged by a u-shaped platinum wire with nylon fibres for mechanical stabilization. The chamber was mounted on a fixed-stage

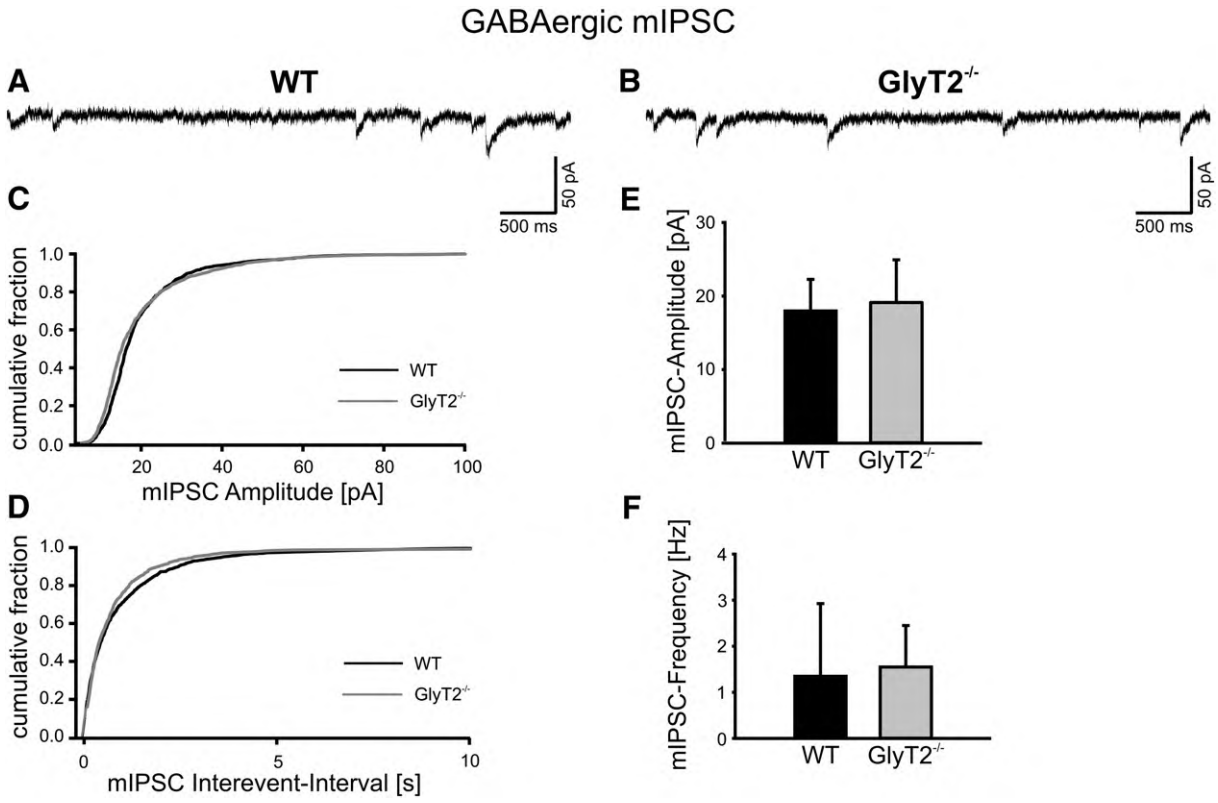

Fig. 6. Normal miniature GABAergic IPSC in GlyT2$^{-/-}$ mice (P3–P5) in the presence of TTX. A, B: No differences between the mean amplitudes of GABAergic mIPSC in both genotypes were detectable. C, D: Additionally the cumulative fractions of the amplitudes and interevent-intervals are almost the same in both WT and GlyT2$^{-/-}$ mice (cut-offs were made for amplitudes at 100 pA and for interevent–intervals at 10 s). E, F: Mean amplitudes (E) and frequencies (F) of miniature IPSC$_{GABA}$ (±SD). The aCSF contained 100 µM AP-5, 20 µM CNQX, 10 µM strychnine, 500 nM TTX, 1 µM zolpidem and 100 mM sucrose during the experiments.

microscope (Zeiss Axioscope, Germany) and continuously perfused with aCSF (room temperature; 20–23 °C) at a flow rate of 4–7 ml/min.

The aCSF contained (in mM): 118 NaCl, 3 KCl, 1.5 $CaCl_2$, 1 $MgCl_2$, 1 NaH_2PO_4, 25 $NaHCO_3$, and 30 D-glucose. The osmolarity of the aCSF was 310 mosm/l, and pH was adjusted to 7.4 with NaOH. sIPSC$_{gly}$ or sIPSC$_{GABA}$ were isolated by adding 20 µM 6-cyano-7-nitroquinoxaline-2,3-dione (CNQX), 100 µM DL-2-amino-5-phosphonopentanoate (AP5, Alexis) and 20 µM bicuculline or 10 µM strychnine, respectively. For detection of mIPSC$_{GABA}$ 500 nM Tetrodotoxin (TTX, Alomone labs), 1 µM Zolpidem and 100 mM Sucrose was added to increase the amplitude and frequency of mIPSC$_{GABA}$ (Perrais and Ropert, 1999; Rosenmund and Stevens, 1996). All drugs were obtained from Sigma (St. Louis, MO, USA) or Tocris Bioscience (Ellisville, MO, USA) if not indicated otherwise.

Hypoglossal motoneurons were visually identified by their localization, size and shape. Whole-cell voltage-clamp recordings were obtained with patch-clamp amplifiers L/M-PCA (E.S.F, Friesland, Germany), Multiclamp 700 (Axon Instruments, Foster City, CA), or EPC9 (Heka, Lambrecht, Germany). Recording electrodes were pulled from borosilicate glass capillaries (Biomedical Instruments, Zöllnitz, Germany) on a horizontal pipette-puller (Zeitz, Munich, Germany). Electrodes had resistances ranging from 2 to 4 MΩ when filled with intracellular solution containing (in mM): 110 CsCl, 30 TEA-Cl, 1 $CaCl_2$, 2 $MgCl_2$, 4 Na_2ATP, 10 HEPES, 10 EGTA (pH was adjusted to 7.2 using KOH). 5-Lidocaine-N-ethyl bromide (QX-314, 5 mM) was added to the electrode solution to block fast voltage-dependent sodium currents. Hypoglossal motoneurons were voltage-clamped at a holding potential of −70 mV. Since the equilibrium potential of chloride was close to 0 mV, IPSCs where recorded as inward currents. Currents were filtered at 3 kHz with a four-pole Bessel filter and digitized at 10 kHz using a PowerLab interface and Chart 5 software (ADInstruments Pty. Ltd., Mountain View, CA). Data were stored on hard disk for offline analysis. IPSC amplitude and frequency was analyzed using the MiniAnalysis program (Jaejin Software, Leonia, NJ) as described earlier (Gomeza et al., 2003b). To minimize fitting errors resulting from noise, decay kinetics of spontaneous IPSCs were calculated from IPSCs with amplitudes that were larger than the mean of the respective experiment. Miniature IPSC kinetics were averaged from all detectable events, independent from their amplitudes, to increase the number of analysed events. Furthermore, only IPSC, which were clearly separated from each other were used. Decay phases were fitted by two exponentials, and the mean time constant, τ_{decay}, was calculated from the respective time constants and their relative amplitudes (a_1,a_2): $\tau_{decay} = \tau_1 a_1 + \tau_2 a_2$ using the MiniAnalysis Program (Hirzel et al., 2006).

Evoked GABAergic inhibitory postsynaptic potentials (eIPSC$_{GABA}$) were recorded after presynaptic electrical stimulation using a concentric bipolar stimulation electrode (WPI, Sarasota, FL), which was placed in the Nucleus of Roller, where somata of inhibitory interneurons projecting to the hypoglossal nucleus are localized. To reach maximal numbers of presynaptic neurons, supra maximal stimulation intensities were achieved by increasing the amplitude (5–20 V) of the constant voltage stimulation pulses (50–100 µs pulse length) until no further increase of the eIPSC$_{GABA}$ amplitude was detectable. Paired-pulses stimulation was performed with intervals of 25 ms to 400 ms (frequency of 2.5 to 40 Hz; see Fig. 5). Three repetitions (~2 s interval) were averaged using Igor Pro 3.1B01 (WaveMetrics Oregon, USA). Additionally to the paired-pulse-ratio (second eIPSC (a_2) divided by the first (a_1)), the peak current after the second stimulus ($a_{2,\,total}$) was used to calculate the ratio $a_{2\,total}/a_1$ (see Fig. 5).

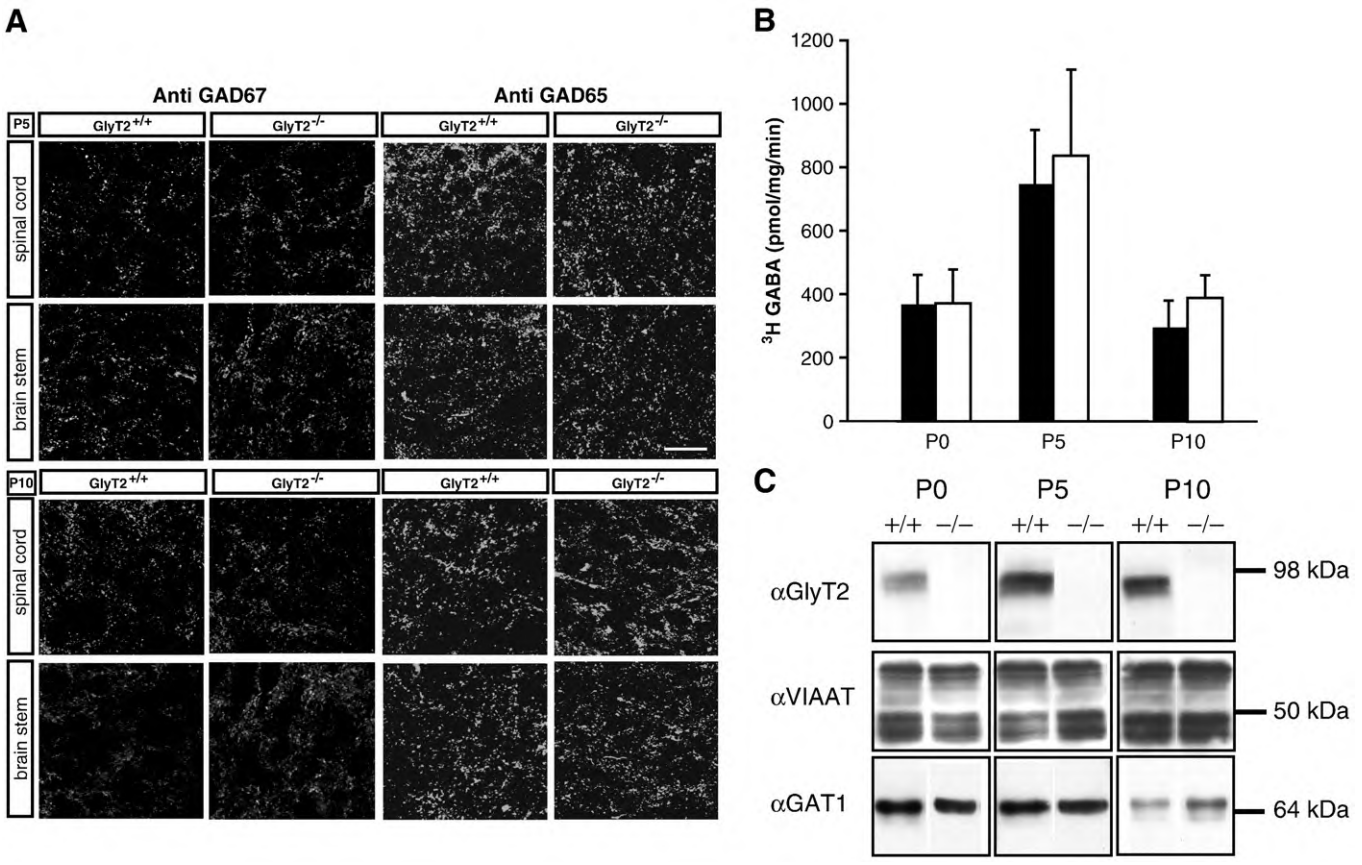

Fig. 7. Normal protein expression at GABAergic synapses in GlyT2$^{-/-}$ mice. A: Brainstem and spinal cord of GlyT2$^{-/-}$ mice and WT litter mates were dissected at the age indicated and after fixation and sectioning stained with antibodies against GAD67 and GAD65 (scale bar represents 20 µm) B: GAT1 specific uptake determined as the tiagabine sensitive uptake in P2 membrane preparations of brainstem. The uptake was measured in preparations from WT (black bars), and GlyT2$^{-/-}$ littermates (open bars), at three different timepoints (P0, P5 and P10). GAT1 specific uptake was 40–60% of the total GAT activity measured in this preparation. C: Analysis of protein expression in P2 membrane preparations of GlyT2, VIAAT and GAT1 at P0, P5 and P10 of WT and GlyT2$^{-/-}$ mice. The expression levels of GAT1 and VIAAT are comparable in the different genotypes, whereas the amount of GlyT2 is not detectable in the knockout mice.

Immunohistochemistry

Neonatal mice were killed by decapitation, the brain and spinal cord was removed and rinsed briefly with ice-cold PBS (in mM: 137 NaCl, 3 KCl, 6.5 Na_2HPO_4, 1.5 KH_2PO_4, pH 7.4). The brain was fixed for 24 h with 4% paraformaldehyde in PBS. After cryoprotection with 30% sucrose in PBS the tissue was frozen on dry ice. 12 µm cryostat slices were prepared from the frozen tissue and stored until use at −80 °C. For stainings with VIAAT and/or Gephyrin specific antibodies, sections were washed twice for 2 min in PBS and once with SC buffer (10 mM sodium citrate, 0.05% (v/v) Tween-20, pH 8.0). Sections were immersed in a pre-heated staining dish containing SC buffer and incubated for 30 min at 95 °C. After allowing the slides to cool at room temperature for 20 min, sections were rinsed twice for 2 min in PBS. For all stainings sections were permeabilized with 0.3% (w/v) Triton X-100, 4% (v/v) goat serum in PBS, blocked for 3 h with 10% (v/v) goat serum in PBS and incubated overnight at 4 °C with the primary antibodies as indicated in PBS/10% goat serum. Bound antibodies were visualized with fluorescence-conjugated antibodies. The antibodies used were raised against VIAAT (1:1000, rabbit, polyclonal, kindly provided by Dr. Bruno Gasnier, Institut de Biologie Physico-Chimique, Paris, France), GAD65 (1:250, mouse monoclonal, Millipore, Temecula, USA), GABA (1:2000, rabbit polyclonal, Sigma, St. Louis, USA), GAD67 (1:1000, mouse monoclonal, Millipore), glycine (rat polyclonal, kindly provided by David Pow, University of Newcastle, Callaghan, Australia) and Gephyrin (mouse monoclonal, 1:500, (Pfeiffer et al., 1984)). Images were acquired using a Zeiss AxioImager microscope equipped with an Apotome or a Leica laser scanning microscope. For quantification, respective immunreactive puncta with sizes between 0.6 µm and 1.5 µm were counted manually. For each staining at least 1000 immunreactive clusters were counted.

Table 2
Quantification of VIAAT and GAT1 immunreactivities (Western-blot).

	GlyT2$^{+/+}$	GlyT2$^{-/-}$
P0		
VIAAT	100 ± 5	112 ± 18
GAT1	100 ± 12	98 ± 15
P5		
VIAAT	100 ± 18	105 ± 11
GAT1	100 ± 7	109 ± 6
P10		
VIAAT	100 ± 9	103 ± 14
GAT1	100 ± 11	97 ± 15

Western blots of P2 membrane preparations derived from WT and GlyT2$^{-/-}$ animals were probed with the indicated antibodies. For quantification, Western blots were scanned and immunoreactive bands subsequently quantified using Image J. Data represent $n \geq 4$. None of the mutant values differ significantly from wild-type levels.

Uptake experiments in P2 membrane preparation

Mice were killed at the indicated age and brainstem and spinal cord were dissected and homogenized in membrane isolation buffer (0.33 M sucrose, 1 mM EDTA, 1 mM PMSF, 10 mM HEPES/Tris, pH 7.5) using a

glass-teflon homogenizer and centrifuged at 4 °C and 1000 *g*. The supernatant was collected and centrifuged at 4 °C and 10,000 *g*. Pellets were resuspended in Krebs–Henseleit–Buffer (KHP, 125 mM NaCl, 5 mM KCl, 2.7 mM $CaCl_2$, 1.3 mM $MgSO_4$, 10 mM glucose and 25 mM HEPES/Tris, pH 7.4), centrifuged at 4 °C and 10,000 *g* resuspended in KHP and stored on ice (P2). For the uptake experiments 20 µl of this suspension was mixed with 80 µl prewarmed KHP and incubated with or without 5 µM tiagaine (5 fold IC50 of GAT1) at 37 °C for 5 min. The incorporation experiment was started by addition of 100 µl prewarmed KHP containing 20 µM GABA and 20 nM [^{3}H]GABA. After 1 min, incorporation was terminated by the addition of 5 ml ice-cold KHP and rapid filtration using a 0.45 µM cellulose acetate filter (Sartorius, Göttingen, Germany). The filter was washed once using 5 ml ice-cold KHP and the incorporation of GABA was analyzed by liquid scintillation counting. GAT1 specific uptake was determined as the fraction of tiagabine sensitive uptake. All measurements were performed as triplicates.

Western blotting

For Western blot analysis, P2 membrane preparations from brainstem and spinal cord of GlyT2 deficient mice and their WT litters were isolated at the indicated time points as described above and subjected to SDS-PAGE and Western blotting. Per lane 25 µg of total protein were used. Western blots were probed with antibodies against GAT1 (rabbit, 1:1000, Millipore), GlyT2 (rabbit, 1:2000, Gomeza et al., 2003b) and VIAAT (rabbit, 1:2000, Synaptic Systems). After washing, bound Igs were visualized with horseradish peroxidase-conjugated secondary antibodies using the ECL detection system (Thermo Scientific, Rockford, IL). The Western blots were scanned and digitalized images were analyzed for quantification using the software ImageJ.

Data analysis

Electrophysiological data were stored on a personal computer for later analysis with MiniAnalysis program (Jaejin Software, Leonia, NJ) and SigmaPlot/SigmaStat (Systat Software, Point Richmond, CA). The unpaired *t*-test or the Mann–Whitney Rank Sum test was used to determine the significance of changes when comparing unpaired values obtained from GlyT2$^{-/-}$ and WT mice. To test for significance of paired-pulse-facilitation the paired *t*-test was used. Results were expressed as mean ± standard deviation (SD), and differences were considered significant if $p \leq 0.05$.

Acknowledgments

We would like to thank Bruno Gasnier and David Pow for providing antibodies, Maren Krause, Anja-Annett Grützner for excellent technical assistance and Heinrich Betz, Cord-Michael Becker and Diethelm W. Richter for their continuous interest in this work. Special thanks go to Peter M. Lalley for the critical reading of the manuscript. This work was supported by the Max Planck Gesellschaft and by the Deutsche Forschungsgemeinschaft through the DFG Research Center Molecular Physiology of the Brain (CMPB).

References

Burger, P.M., Hell, J., Mehl, E., Krasel, C., Lottspeich, F., Jahn, R., 1991. GABA and glycine in synaptic vesicles: storage and transport characteristics. Neuron 7, 287–293.

Chaudhry, F.A., Reimer, R.J., Bellocchio, E.E., Danbolt, N.C., Osen, K.K., Edwards, R.H., Storm-Mathisen, J., 1998. The vesicular GABA transporter, VGAT, localizes to synaptic vesicles in sets of glycinergic as well as GABAergic neurons. J. Neurosci. 18, 9733–9750.

Christensen, H., Fonnum, F., 1991. Uptake of glycine, GABA and glutamate by synaptic vesicles isolated from different regions of rat CNS. Neurosci. Lett. 129, 217–220.

Christensen, H., Fykse, E.M., Fonnum, F., 1991. Inhibition of gamma-aminobutyrate and glycine uptake into synaptic vesicles. Eur. J. Pharmacol. 207, 73–79.

Conti, F., Melone, M., De Biasi, S., Minelli, A., Brecha, N.C., Ducati, A., 1998. Neuronal and glial localization of GAT-1, a high-affinity gamma-aminobutyric acid plasma membrane transporter, in human cerebral cortex: with a note on its distribution in monkey cortex. J. Comp. Neurol. 396, 51–63.

Daly, E.C., Aprison, M.H., 1974. Distribution of serine hydroxymethyltransferase and glycine transaminase in several areas of the central nervous system of the rat. J. Neurochem. 22, 877–885.

Eulenburg, V., Becker, K., Gomeza, J., Schmitt, B., Becker, C.M., Betz, H., 2006. Mutations within the human GLYT2 (SLC6A5) gene associated with hyperekplexia. Biochem. Biophys. Res. Commun. 348, 400–405.

Feng, G., Tintrup, H., Kirsch, J., Nichol, M.C., Kuhse, J., Betz, H., Sanes, J.R., 1998. Dual requirement for gephyrin in glycine receptor clustering and molybdoenzyme activity. Science 282, 1321–1324.

Gomeza, J., Hulsmann, S., Ohno, K., Eulenburg, V., Szoke, K., Richter, D., Betz, H., 2003a. Inactivation of the glycine transporter 1 gene discloses vital role of glial glycine uptake in glycinergic inhibition. Neuron 40, 785–796.

Gomeza, J., Ohno, K., Hulsmann, S., Armsen, W., Eulenburg, V., Richter, D.W., Laube, B., Betz, H., 2003b. Deletion of the mouse glycine transporter 2 results in a hyperekplexia phenotype and postnatal lethality. Neuron 40, 797–806.

Hirzel, K., Muller, U., Latal, A.T., Hulsmann, S., Grudzinska, J., Seeliger, M.W., Betz, H., Laube, B., 2006. Hyperekplexia phenotype of glycine receptor alpha1 subunit mutant mice identifies Zn(2+) as an essential endogenous modulator of glycinergic neurotransmission. Neuron 52, 679–690.

Jensen, K., Chiu, C.S., Sokolova, I., Lester, H.A., Mody, I., 2003. GABA transporter-1 (GAT1)-deficient mice: differential tonic activation of GABAA versus GABAB receptors in the hippocampus. J. Neurophysiol. 90, 2690–2701.

Jin, H., Wu, H., Osterhaus, G., Wei, J., Davis, K., Sha, D., Floor, E., Hsu, C.C., Kopke, R.D., Wu, J.Y., 2003. Demonstration of functional coupling between gamma -aminobutyric acid (GABA) synthesis and vesicular GABA transport into synaptic vesicles. Proc. Natl Acad. Sci. USA 100, 4293–4298.

Jonas, P., Bischofberger, J., Sandkuhler, J., 1998. Corelease of two fast neurotransmitters at a central synapse. Science 281, 419–424.

Kneussel, M., Loebrich, S., 2007. Trafficking and synaptic anchoring of ionotropic inhibitory neurotransmitter receptors. Biol. Cell / Auspices Eur. Cell Biol. Org. 99, 297–309.

Lu, T., Rubio, M.E., Trussell, L.O., 2008. Glycinergic transmission shaped by the corelease of GABA in a mammalian auditory synapse. Neuron 57, 524–535.

Mahendrasingam, S., Wallam, C.A., Hackney, C.M., 2000. An immunogold investigation of the relationship between the amino acids GABA and glycine and their transporters in terminals in the guinea-pig anteroventral cochlear nucleus. Brain Res. 887, 477–481.

Mangin, J.M., Guyon, A., Eugene, D., Paupardin-Tritsch, D., Legendre, P., 2002. Functional glycine receptor maturation in the absence of glycinergic input in dopaminergic neurones of the rat substantia nigra. J. Physiol. 542, 685–697.

McIntire, S.L., Reimer, R.J., Schuske, K., Edwards, R.H., Jorgensen, E.M., 1997. Identification and characterization of the vesicular GABA transporter. Nature 389, 870–876.

Minelli, A., Brecha, N.C., Karschin, C., DeBiasi, S., Conti, F., 1995. GAT-1, a high-affinity GABA plasma membrane transporter, is localized to neurons and astroglia in the cerebral cortex. J. Neurosci. 15, 7734–7746.

Mintz, I.M., Bean, B.P., 1993. GABAB receptor inhibition of P-type Ca^{2+} channels in central neurons. Neuron 10, 889–898.

Misgeld, U., Bijak, M., Jarolimek, W., 1995. A physiological role for GABAB receptors and the effects of baclofen in the mammalian central nervous system. Prog. Neurobiol. 46, 423–462.

Muller, E., Le Corronc, H., Triller, A., Legendre, P., 2006. Developmental dissociation of presynaptic inhibitory neurotransmitter and postsynaptic receptor clustering in the hypoglossal nucleus. Mol. Cell. Neurosci. 32, 254–273.

O'Brien, J.A., Berger, A.J., 1999. Cotransmission of GABA and glycine to brain stem motoneurons. J. Neurophysiol. 82, 1638–1641.

Perrais, D., Ropert, N., 1999. Effect of zolpidem on miniature IPSCs and occupancy of postsynaptic GABAA receptors in central synapses. J. Neurosci. 19, 578–588.

Pfeiffer, F., Simler, R., Grenningloh, G., Betz, H., 1984. Monoclonal antibodies and peptide mapping reveal structural similarities between the subunits of the glycine receptor of rat spinal cord. Proc. Natl Acad. Sci. USA 81, 7224–7227.

Pow, D.V., Wright, L.L., Vaney, D.I., 1995. The immunocytochemical detection of amino-acid neurotransmitters in paraformaldehyde-fixed tissues. J. Neurosci. Meth. 56, 115–123.

Rees, M.I., Lewis, T.M., Kwok, J.B., Mortier, G.R., Govaert, P., Snell, R.G., Schofield, P.R., Owen, M.J., 2002. Hyperekplexia associated with compound heterozygote mutations in the beta-subunit of the human inhibitory glycine receptor (GLRB). Hum. Mol. Genet. 11, 853–860.

Rees, M.I., Harvey, K., Pearce, B.R., Chung, S.K., Duguid, I.C., Thomas, P., Beatty, S., Graham, G.E., Armstrong, L., Shiang, R., Abbott, K.J., Zuberi, S.M., Stephenson, J.B., Owen, M.J., Tijssen, M.A., van den Maagdenberg, A.M., Smart, T.G., Supplisson, S., Harvey, R.J., 2006. Mutations in the gene encoding GlyT2 (SLC6A5) define a presynaptic component of human startle disease. Nat. Genet. 38, 801–806.

Rosenmund, C., Stevens, C.F., 1996. Definition of the readily releasable pool of vesicles at hippocampal synapses. Neuron 16, 1197–1207.

Rousseau, F., Aubrey, K.R., Supplisson, S., 2008. The glycine transporter GlyT2 controls the dynamics of synaptic vesicle refilling in inhibitory spinal cord neurons. J. Neurosci. 28, 9755–9768.

Sagne, C., El Mestikawy, S., Isambert, M.F., Hamon, M., Henry, J.P., Giros, B., Gasnier, B., 1997. Cloning of a functional vesicular GABA and glycine transporter by screening of genome databases. FEBS Lett. 417, 177–183.

Shiang, R., Ryan, S.G., Zhu, Y.Z., Hahn, A.F., O'Connell, P., Wasmuth, J.J., 1993. Mutations in the alpha 1 subunit of the inhibitory glycine receptor cause the dominant neurologic disorder, hyperekplexia. Nat. Genet. 5, 351–358.

Singer, J.H., Berger, A.J., 2000. Development of inhibitory synaptic transmission to motoneurons. Brain Res. Bull. 53, 553–560.
Singer, J.H., Talley, E.M., Bayliss, D.A., Berger, A.J., 1998. Development of glycinergic synaptic transmission to rat brainstem motoneurons. J. Neurophysiol. 80, 2608–2620.
Stil, A., Liabeuf, S., Jean-Xavier, C., Brocard, C., Viemari, J.C., Vinay, L., 2009. Developmental up-regulation of the potassium-chloride cotransporter type 2 in the rat lumbar spinal cord. Neuroscience 164, 809–821.
Tanabe, M., Kaneko, T., 1996. Paired pulse facilitation of GABAergic IPSCs in ventral horn neurons in neonatal rat spinal cord. Brain Res. 716, 101–106.
Wojcik, S.M., Katsurabayashi, S., Guillemin, I., Friauf, E., Rosenmund, C., Brose, N., Rhee, J.S., 2006. A shared vesicular carrier allows synaptic corelease of GABA and glycine. Neuron 50, 575–587.
Zafra, F., Aragon, C., Olivares, L., Danbolt, N.C., Gimenez, C., Storm-Mathisen, J., 1995. Glycine transporters are differentially expressed among CNS cells. J. Neurosci. 15, 3952–3969.
Zhang, W., Barnbrock, A., Gajic, S., Pfeiffer, A., Ritter, B., 2002. Differential ontogeny of GABA(B)-receptor-mediated pre- and postsynaptic modulation of GABA and glycine transmission in respiratory rhythm-generating network in mouse. J. Physiol. 540, 435–446.